# DESIGNING OF PHASE II ARL-UNBIASED $S^2$-CHART WITH IMPROVED PERFORMANCE USING REPETITIVE SAMPLING

Sonam Jaiswal[1] and Nirpeksh Kumar[2*]

•

[1]DST-Center for Interdisciplinary Mathematical Sciences (DST-CIMS), Banaras Hindu University, Uttar Pradesh, India

[2*]Department of Statistics, Banaras Hindu University, Uttar Pradesh, India

[1]jsonam572@gmail.com

[2*]nirpeksh@gmail.com

**Abstract**

*In this paper, we consider a two-sided Phase II $S^2$-chart with probability limits because the surveillance of both an increase and decrease in the process variance plays a decisive role in a continuous quality improvement program. We propose a two-sided average run length unbiased $S^2$-chart under the repetitive sampling with probability limits for a fixed in-control average run length and average sample size to eliminate the average run length biasedness. It is well established that the Shewhart-type charts are less sensitive to detect small to moderate changes in the process parameters. Therefore, a repetitive sampling scheme is taken into consideration to improve the $S^2$-chart's ability to detect changes in the process variance. Under the repetitive sampling methodology, the detection ability of the chart is improved by using more than one samples if the first sample does not provide sufficient evidence to decide whether the process is in-control or out-of-control. The proposed chart is compared with the existing charts, such as the equal tailed standard Shewhart $S^2$-chart and unequal tailed $S^2$-chart under repetitive sampling. Results show that the proposed chart is more efficient than the existing chart. Finally, an illustration has been provided in the favor of the proposed chart with the help of a published dataset.*

**Keywords:** Average run length, average sample number, average run length-unbiased, Control chart, in-control and out-of-control performances, Process variability.

## 1. Introduction

Recently, the $S^2$-chart has gained popularity to monitor a decrease and increase in the process variability when the quality characteristic is normally distributed. On the other hand, the traditional control charts, such as $R$- and $S$-charts with symmetric control limits, have some shortcomings. For example, the negative lower control limits are found for small sample sizes $n$ ($n \leq 5$ for the $R$-chart and $n \leq 6$ for the $S$-chart), and their in-control (IC) performance significantly differs from the IC

* Corresponding author. Nirpeksh Kumar. Email: nirpeksh@gmail.com

performance expected one. See Knoth and Morais [13] and references therein for a detailed discussion on the limitations of the $R$- and $S$-charts with symmetric limits. In fact, the $R$ and $S$-charts with symmetric control limits are less sensitive to detect a decrease in the process variance which refers to an improvement case whereas perform satisfactorily to detect an increase in the process variance. Nevertheless, in many situations, it is of interest to know the factors which are responsible for a low process variability so that a new standard can be set for the forthcoming production. Sarmiento, Chakraborti and Epprecht [17] have discussed, however, in the context of statistical tolerance limits to assess the product quality, that lowering the process variability is one of the most important objectives in the quality control studies.

For the $S^2$-chart, several efforts have been made to increase the efficacy of detecting the upward and downward changes in the process variance. For example, using memory-type charts such as exponentially weighted moving average (EWMA) and cumulative sum (CUSUM) charts (see Chang and Gan [8, 9], Castagliola, Celano and Fichera [7], Lawson [14], and references therein). Besides these, the ability of the charts to detect changes can also be improved by using more than one sample if the first sample does not provide sufficient evidence to decide whether the process is IC or out-of-control (OOC). The idea is derived from the acceptance sampling plan, where the following sample is considered when the decision of rejecting or accepting a lot cannot be made based on the first sample. The different strategies are considered to use the information from the next sample. For example, in a double sampling plan, a second sample is used if the decision is not made on the first sample, and combined information of both samples is used to take a decision (see Montgomery [15]). Various attempts to design the charts based on double sampling are made to improve the chart's ability to detect OOC signals. See, for example, S-chart for agile manufacturing (He and Grigoryan [11]), $S^2$-chart (Khoo [12]).

In recent years, the repetitive sampling (RS) has been used to design charts by several authors, to name a few; see Ahmad, Aslam and Jun [1], Aslam, Azam, and Jun [4], Aslam, Khan, Azam et al. [6]. The idea of the RS was firstly used by Sherman [18] to develop an attribute acceptance sampling plan. In order to implement the RS to the control chart, the region of the control chart is divided into three sub-regions: the acceptance region (IC region), the indecision region (repetitive region), and the rejection region (OOC region). The quality control personnel use the next sample when the first plotted sample falls in the indecision region and repeats the process until the sample lies either in the acceptance or rejection region. Please note here that in the RS scheme, we do not keep track of how many times we have repeated our sample. Thus, under the RS scheme, on average, more than one charting point is required to make a final decision on IC or OOC status of the process. This is usually measured by the average sample size (ASS) (the expected number of sample size needed until the final decision is made) that can be fixed in advance. In addition, this scheme uses fewer number of parameters to design a control chart based on double sampling (Aslam, Azam and Jun [4], Aslam, Khan, Azam et al. [6]). Moreover, in comparison to other sampling schemes, the RS scheme throws information away by discarding the samples lying in the indecision region. Still, on the other hand, we gain in the simplicity of design and execution. Ahamd, Aslam, and Jun [1] implemented the RS in constructing the $\bar{X}$ control limits based on the capability index. Aslam, Azam and Jun [4] developed the attribute chart and $np$ chart under the RS. Aslam, Khan, Azam et al. [6] used RS to design the $T$-chart based on the transformed exponential variables. Aslam [3] used the RS to design the $S^2$-chart for the neutrosophic statistic. Recently, Alevizakos, Chatterjee, Koukouvinos et al. [2] examined the effect of parameter estimation on the performance of the variable control charts under the RS and Singh and Kumar [19] designed the average run length (ARL)-unbiased exponential chart under the RS to monitor the inter-arrival times in high-yield processes. Performance of different chart under RS shows better detection ability in the OOC case than the standard one's.

Note that Aslam, Khan and Jun [5] considered the RS to propose a new $S^2$-chart with equal

distance (3-sigma) limits (thereafter AKJ chart) and showed superior to the existing standard $S^2$-chart. Note that they constructed the two-sided chart, but discussed only the case of process deterioration (increased variance). But to have an idea about their chart's performance in the improvement case, we calculated the ARL values using their control limits for shifts representing the improvement case (decreased variance). It is worth to mention here that the chart with equal-tailed limits and using a skewed charting statistic possesses an undesirable property which is known as ARL-biased in the SPC literature. For such (ARL-biased) charts, the ARL function does not achieve its maximum at the IC state. As a result, the chart gives a delayed OOC signal than the false alarm. For more details, please refer to Knoth and Morais [13], Zhang, Bebbington, Lai et al. [20]. To overcome this property, the ARL-unbiased charts are proposed to ensure the detection of shifts in the process parameter more quickly than a false alarm. Note that Aslam, Khan and Jun [5] designed chart is ARL-biased and triggers an OOC signal lately for a decrease in the process variance than it raises a false alarm. However, Knoth and Morais [13] point out that a decrease in the process variance should be followed seriously as it is a synonym for a quality improvement. Thus, the adoption of ARL-unbiased charts can play an absolutely deciding role in achieving the final goal of producing better-quality items (Pignatiello et al. [16]), while using charts to signal to both decreases and increases in a parameter.

The objective of this study is to improve the ability of the Phase II two-sided ARL-biased and ARL-unbiased $S^2$-chart to detect an increase and decrease in the process variance by implementing the RS scheme and to compare their performances with the existing the AKJ chart and the standard ARL-biased and -unbiased $S^2$- charts.

The rest of the article is organized as follows. Section 2 discusses a general charting procedure to construct the equal-tailed $S^2$-chart under the RS. In section 3, the performances of the proposed $S^2$-chart under the RS are examined and compared with the AKJ and standard $S^2$-charts. In section 4, we design the ARL-unbiased $S^2$-chart under the RS and its performance is evaluated in Section 5. An example is provided in Section 6. Finally, the concluding remarks are offered in Section 7.

## 2. Phase II $S^2$-chart with equal-tailed probability limits under repetitive sampling

Let $X_1, X_2, \ldots, X_n$ be independently and identically distributed $N(\mu, \sigma_0^2)$ random variables where $\mu$ and $\sigma_0^2$ are the IC process mean and variance, respectively. The charting statistic for the $S^2$-chart is the sample variance given by $S^2 = \frac{1}{n-1}\sum_{j=1}^{n}\left(X_j - \bar{X}\right)^2, \bar{X} = \frac{1}{n}\sum_{j=1}^{n} X_j$. Let LCL and UCL be the lower and upper control limits, respectively, of the standard $S^2$-chart (with the single sampling (SS) scheme). Thus, the equal-tailed limits can be obtained from $P[S^2 < \text{LCL}|\sigma_0^2] = P[S^2 > \text{UCL}|\sigma_0^2] = \frac{\alpha}{2}$, where $\alpha$ is the nominal false alarm rate (FAR). It is known that $(n-1)S^2/\sigma_0^2$ follows a $\chi^2$-distribution with $(n-1)$ degrees of freedom (df). Thus, the control limits LCL and UCL can be expressed as follows.

$$\text{LCL} = \frac{\sigma_0^2}{n-1}\chi^2_{\frac{\alpha}{2},n-1} = \frac{\sigma_0^2}{n-1}A_1 \quad \text{and} \quad \text{UCL} = \frac{\sigma_0^2}{n-1}\chi^2_{1-\frac{\alpha}{2},n-1} = \frac{\sigma_0^2}{n-1}A_2 \tag{1}$$

where $A_1 = \chi^2_{\frac{\alpha}{2},n-1}$, $A_2 = \chi^2_{1-\frac{\alpha}{2},n-1}$. The $\chi^2_{\zeta,n-1}$ denotes the $100\zeta$-percentile of the $\chi^2$-distribution with $(n-1)$ df. The center line (CL) of the $S^2$-chart is given by

$$\text{CL} = \frac{\sigma_0^2}{n-1}\chi^2_{0.5,n-1} = \frac{\sigma_0^2}{n-1}A_3 \tag{2}$$

where $\text{A}_3 = \chi^2_{0.5,n-1}$. Define $\delta = \frac{\sigma_1^2}{\sigma_0^2} > 0$, which quantifies the magnitude of the process variance shift from IC variance $\sigma_0^2$ to the shifted variance $\sigma_1^2 = \delta\sigma_0^2$. Clearly, for $\delta = 1$, the process is IC, otherwise it is OOC. Further note that $\delta > 1$ ($\delta < 1$) represents the upward (downward) shift in the process variance reflecting the increased (decreased) process variability which refers to the deterioration (improvement) case. Let us define a signalling event $E$ that the charting statistic lies outside the control limits. Thus, the probability of signal (PS), when the process variance is $\sigma_1^2$, is given by

$$\beta(\delta) = \mathrm{P}(E|\sigma_1^2) = P[S^2 < \mathrm{LCL} \text{ or } S^2 > \mathrm{UCL}|\sigma_1^2 = \delta\sigma_0^2]$$
$$= 1 + F_{\chi^2_{n-1}}\left(\frac{A_1}{\delta}\right) - F_{\chi^2_{n-1}}\left(\frac{A_2}{\delta}\right)$$

where $F_{\chi^2_{n-1}}(\cdot)$ denotes the cumulative distribution function (CDF) of the $\chi^2$-distribution with $(n-1)$ df. Thus, the ARL, the reciprocal of the PS, for a Shewhart chart, is given by

$$\mathrm{ARL}(\delta) = \frac{1}{\beta((\delta)} \tag{3}$$

To implement the RS, in addition to the outer control limits, say, $\mathrm{UCL_{RS}}, \mathrm{LCL_{RS}}$, two additional inner (repetitive) control limits $\mathrm{URL_{RS}}$ and $\mathrm{LRL_{RS}}$ are introduced. Consequently, the whole area of the control chart is divided into six regions which are as follows- (i) one extending above the $\mathrm{UCL_{RS}}$ (region $a$), (ii) one extending between $\mathrm{UCL_{RS}}$ and $\mathrm{URL_{RS}}$ (region $b$), (iii) one extending between $\mathrm{URL_{RS}}$ and $\mathrm{CL}$ (region $c$), (iv) one extending between the $\mathrm{CL}$ and $\mathrm{LRL_{RS}}$ (region $d$), (v) one extending between $\mathrm{LRL_{RS}}$ and $\mathrm{LCL_{RS}}$ (region $e$), (vi) one extending below $\mathrm{LCL_{RS}}$ (region $f$). These six regions can further be broadly classified as OOC region (regions $(a)$ and $(f)$), indecision region (regions $(b)$ and $(e)$) and the IC region (regions $(c)$ and $(d)$), respectively. The control limits are such that $\mathrm{UCL_{RS}} \geq \mathrm{URL_{RS}} > \mathrm{CL} > \mathrm{LRL_{RS}} \geq \mathrm{LCL_{RS}}$. Under the RS, the process is declared to be OOC (IC), when the charting point lies in the OOC region (IC region). Otherwise, the process is repeated for the resampling when the charting point lies in the indecision region. Let $\alpha_1$ and $\alpha_2$ be the probabilities of a charting point lying beyond the $\mathrm{UCL_{RS}}$ and $\mathrm{LCL_{RS}}$, and $\mathrm{URL_{RS}}$ and $\mathrm{LRL_{RS}}$, respectively. Thus, the equal-tailed outer and inner control limits can be obtained from $P[S^2 < \mathrm{LCL_{RS}}|\sigma_0^2] = P[S^2 > \mathrm{UCL_{RS}}|\sigma_0^2] = \alpha_1/2$ and $P[S^2 < \mathrm{LRL_{RS}}|\sigma_0^2] = P[S^2 > \mathrm{URL_{RS}}|\sigma_0^2] = \alpha_2/2$, which can be obtained as follows.

$$\mathrm{LCL_{RS}} = \frac{\sigma_0^2}{n-1}\chi^2_{\alpha_1/2,n-1} = \frac{\sigma_0^2}{n-1}B_1 \quad \text{and} \quad \mathrm{UCL_{RS}} = \frac{\sigma_0^2}{n-1}\chi^2_{1-\alpha_1/2,n-1} = \frac{\sigma_0^2}{n-1}B_2 \tag{4a}$$

$$\mathrm{LRL_{RS}} = \frac{\sigma_0^2}{n-1}\chi^2_{\alpha_2/2,n-1} = \frac{\sigma_0^2}{n-1}R_1 \quad \text{and} \quad \mathrm{URL_{RS}} = \frac{\sigma_0^2}{n-1}\chi^2_{1-\alpha_2/2,n-1} = \frac{\sigma_0^2}{n-1}R_2 \tag{4b}$$

The constants $\alpha_1$ and $\alpha_2$ $(0 < \alpha_1 \leq \alpha_2 < 1)$ are known as design constants for the $S^2$-chart under the RS. Note that for the RS scheme, we must have $\alpha_1 < \alpha_2$, otherwise, the $\alpha_1 = \alpha_2$ will result in $\mathrm{UCL_{RS}} = \mathrm{URL_{RS}}$ and $\mathrm{LCL_{RS}} = \mathrm{LRL_{RS}}$. As a result, the control chart under the RS reduces to the standard $S^2$-chart in Equation (1). Let $p_a, p_b, p_c, p_d, p_e$ and $p_f$ denote the probabilities of a charting point lying in regions $a, b, c, d, e$, and $f$, respectively. Then, for a shift $\delta > 0$, and using Equations (2) and (4), these probabilities can be calculated as follows.

$$p_a(\delta) = P[S^2 \in a|\sigma_1^2] = P[S^2 > \mathrm{UCL_{RS}}|\sigma_1^2] = 1 - F_{\chi^2_{n-1}}\left(\frac{B_1}{\delta}\right), \tag{5a}$$

$$p_b(\delta) = P[S^2 \in b|\sigma_1^2] = P[\mathrm{URL_{RS}} < S^2 \leq \mathrm{UCL_{RS}}|\sigma_1^2] = F_{\chi^2_{n-1}}\left(\frac{B_1}{\delta}\right) - F_{\chi^2_{n-1}}\left(\frac{R_1}{\delta}\right), \tag{5b}$$

$$p_c(\delta) = P[S^2 \in c|\sigma_1^2] = P[\mathrm{CL} < S^2 \leq \mathrm{URL_{RS}}|\sigma_1^2] = F_{\chi^2_{n-1}}\left(\frac{R_1}{\delta}\right) - F_{\chi^2_{n-1}}\left(\frac{A_3}{\delta}\right), \tag{5c}$$

$$p_d(\delta) = P[S^2 \in d|\sigma_1^2] = P[\mathrm{LRL_{RS}} < S^2 \leq \mathrm{CL}|\sigma_1^2] = F_{\chi^2_{n-1}}\left(\frac{A_3}{\delta}\right) - F_{\chi^2_{n-1}}\left(\frac{R_2}{\delta}\right), \tag{5d}$$

$$p_e(\delta) = P[S^2 \in e|\sigma_1^2] = P[\mathrm{LCL_{RS}} < S^2 \leq \mathrm{LRL_{RS}}|\sigma_1^2] = F_{\chi^2_{n-1}}\left(\frac{R_2}{\delta}\right) - F_{\chi^2_{n-1}}\left(\frac{B_2}{\delta}\right), \tag{5e}$$

$$p_f(\delta) = P[S^2 \in f|\sigma_1^2] = P[S^2 < \mathrm{LCL_{RS}}|\sigma_1^2] = F_{\chi^2_{n-1}}\left(\frac{B_2}{\delta}\right). \tag{5f}$$

The probability of declaring the process OOC on a single sample is given by

$$\beta_{\mathrm{out}}(\delta) = p_a(\delta) + p_f(\delta),$$

and the probability of repetition (resampling) until the decision made is

$$\beta_{rep}(\delta) = p_b(\delta) + p_e(\delta)$$

Thus, under the RS, the PS is given by (Aslam et al. (2015))

$$\beta_{\mathrm{RS}}(\delta) = \frac{\beta_{\mathrm{out}}(\delta)}{1-\beta_{\mathrm{rep}}(\delta)} = \frac{p_a(\delta)+p_f(\delta)}{1-p_b(\delta)-p_e(\delta)} \tag{6}$$

Clearly, under the RS, the RL will also follow a geometric distribution with parameter, $\beta_{\mathrm{RS}}(\delta)$. Thus, the ARL function of the $S^2$-chart under the RS is given by

$$\mathrm{ARL_{RS}}(\delta) = \frac{1}{\beta_{\mathrm{RS}}(\delta)} = \frac{1-p_b(\delta)-p_e(\delta)}{p_a(\delta)+p_f(\delta)} \tag{7}$$

and the ASS for a given shift $(\delta)$ is given by (Aslam, Khan and Jun [5])

$$\mathrm{ASS}_{\mathrm{RS}}(\delta) = \frac{n}{1-\beta_{\mathrm{rep}}(\delta)} = \frac{n}{1-p_b(\delta)-p_e(\delta)} \quad (8)$$

It follows from Equation (8) that the ASS $= n$ for the chart using the SS whereas $\mathrm{ASS}_{\mathrm{RS}}(1) > n$, for the chart using the RS. Most of the existing works design the control charts under the RS for a fixed nominal IC ARL value, but a possible minimum value of the $\mathrm{ASS}_{\mathrm{RS}}(1)$ under some variations. This provides a subjective selection of the control limits, and each practitioner will have his own control limits. To avoid ambiguity, we fix IC ASS i.e., $\mathrm{ASS}_{\mathrm{RS}}(1)$ in advance and then construct the control limits. The choice of the $\mathrm{ASS}_{\mathrm{RS}}(1)$ depends on the user's own choice that how much he is willing to wait for a decision (large $\mathrm{ASS}_{\mathrm{RS}}(1)$) for a better OOC performance. See Singh and Kumar [35]. Thus, to obtain the design constants $\alpha_1$ and $\alpha_2$ for a fixed IC ARL i.e., $\mathrm{ARL}_{\mathrm{RS}}(1)$ value, say, $\mathrm{ARL}_0$ and IC ASS value, $\mathrm{ASS}_{\mathrm{RS}}(1)$ value, say, $\mathrm{ASS}_0$, we need to solve the following pair of Equations

$$\mathrm{ARL}_{\mathrm{RS}}(1) = \frac{1}{\beta_{\mathrm{RS}}(1)} = \mathrm{ARL}_0 \quad (9a)$$

$$\mathrm{ASS}_{\mathrm{RS}}(1) = \frac{n}{1-\beta_{\mathrm{rep}}(1)} = \mathrm{ASS}_0 \quad (9b)$$

Using the design constants $(\alpha_1, \alpha_2)$, we can obtain the control limits for the $S^2$-chart under the RS. Once we obtain the design constants, we can calculate the control limits of the proposed $S^2$-chart using Equation (4).

## 3. Comparative Study

In this section, we compare the performance of the proposed control chart with the existing standard $S^2$ and the AKJ chart. The performance of the charts are evaluated in terms of the ARL, and lower OOC ARL values are desirable for an efficient chart.

### 3.1 Proposed equal-tailed $S^2$-chart versus Aslam et al. (2015) chart

In order to compare the performances, the ARL values of the AKJ chart (Aslam et al. [5] chart) for $n = 4, \mathrm{ARL}_0 = 370, ASS_0 = 4.11$ and $n = 7, \mathrm{ARL}_0 = 370, ASS_0 = 7.36$ are used. Further, we obtained the ARL values for the proposed chart with keeping similar IC metrics for $n = 4, 7$ i.e., $\mathrm{ARL}_0 = 370$ and $\mathrm{ASS}_0 = 4.11, 7.36$, respectively. These values are presented in Table 1. It can be observed that the AKJ chart outperforms the proposed chart in the deterioration case, however, it is very less sensitive to detect a decrease in the process variance. It is expected that with an increase in the shift size in any direction, the chart's ability to detect the changes must increase. However, the AKJ chart's sensitivity decreases to detect the larger downward shifts which contradicts the philosophy of using the control chart. The AKJ chart is insensitive to detect the improvement in the process and hence the decision of using two-sided chart becomes questionable. Thus, we do not recommend the AKJ chart when the interest lies in both improvement and deterioration cases and the direction of shifts is not known. On the other hand, for the proposed chart, the OOC ARL values decreases as $\delta$ goes far away from $\delta = 1$, except for some $\delta < 1$ values close to one. As we have discussed earlier, it is undesirable and in the following section, we eliminate it.

**Table 1:** *Comparison of proposed chart with the chart by Aslam et al. (2015)*

| | $n = 4$ | | | | | | $n = 7$ | | | | | |
|---|---|---|---|---|---|---|---|---|---|---|---|---|
| | AKJ chart | | Proposed chart | | $S^2$ chart | | AKJ chart | | Proposed chart | | $S^2$ chart | |
| $\delta$ | ARL | ASS | ARL | ASS | ARL | ASS | ARL | ASS | ARL | ASS | ARL | ASS |
| **0.1** | 4.25E+17 | 4.00 | 18.77 | 5.54 | 25.34 | 4.00 | 9.82E+17 | 7.00 | 1.15 | 17.65 | 2.82 | 7.00 |
| **0.3** | 3.46E+09 | 4.00 | 118.22 | 4.31 | 124.14 | 4.00 | 6.76E+11 | 7.00 | 20.59 | 10.19 | 28.69 | 7.00 |

| | | | | | | | | | | | | |
|---|---|---|---|---|---|---|---|---|---|---|---|---|
| **0.5** | 338135.52 | 4.00 | 261.32 | 4.15 | 263.92 | 4.00 | 2589301.43 | 7.00 | 99.43 | 7.98 | 108.14 | 7.00 |
| **0.7** | 6778.54 | 4.02 | 425.98 | 4.10 | 424.74 | 4.00 | 15179.88 | 7.05 | 266.07 | 7.45 | 269.64 | 7.00 |
| **0.9** | 785.32 | 4.07 | 461.51 | 4.10 | 459.62 | 4.00 | 956.87 | 7.22 | 434.79 | 7.33 | 432.65 | 7.00 |
| **1** | 370.00 | 4.11 | 370.00 | 4.11 | 370.00 | 4.00 | 370.00 | 7.36 | 370.00 | 7.36 | 370.00 | 7.00 |
| **1.1** | 199.90 | 4.16 | 260.76 | 4.13 | 262.60 | 4.00 | 171.14 | 7.55 | 241.47 | 7.43 | 244.83 | 7.00 |
| **1.3** | 77.45 | 4.27 | 118.48 | 4.19 | 121.62 | 4.00 | 52.86 | 8.01 | 85.92 | 7.68 | 90.87 | 7.00 |
| **1.5** | 38.59 | 4.39 | 59.34 | 4.27 | 62.27 | 4.00 | 22.59 | 8.52 | 35.93 | 8.03 | 39.95 | 7.00 |
| **1.7** | 22.65 | 4.51 | 33.95 | 4.36 | 36.44 | 4.00 | 11.94 | 9.03 | 18.24 | 8.41 | 21.34 | 7.00 |
| **3** | 4.16 | 5.01 | 5.34 | 4.80 | 6.36 | 4.00 | 2.00 | 10.11 | 2.45 | 9.68 | 3.35 | 7.00 |
| **4** | 2.52 | 5.07 | 3.02 | 4.90 | 3.68 | 4.00 | 1.38 | 9.40 | 1.55 | 9.29 | 2.04 | 7.00 |
| $\boldsymbol{k_1}$ | 4.557690 | | | | | | 4.094190 | | | | | |
| $\boldsymbol{k_2}$ | 2.432020 | | | | | | 1.873700 | | | | | |
| $\boldsymbol{\alpha_1}$ | | | 0.002630 | | 0.001351 | | | | 0.002570 | | 0.001351 | |
| $\boldsymbol{\alpha_2}$ | | | 0.029400 | | 0.001351 | | | | 0.051490 | | 0.001351 | |

## 3.2 Proposed equal tails $S^2$-chart versus equal-tailed (standard) $S^2$-chart

Now, the ARL comparison of the proposed chart and the standard $S^2$-chart is presented. The OOC ARL values for the standard $S^2$-chart are also presented in Table 1. It can be observed that the use of the RS improves the performance of the chart. For example, when $\delta = 1.3$, the ARL values for the proposed chart are 118.48 for $n = 4$ and 85.92 for $n = 7$, respectively whereas these values for the standard $S^2$-chart are 121.62 and 90.87, respectively. In the improvement case ($\delta < 1$), except small shifts sizes, for example, for $0.7 < \delta < 1$ when $n = 4$ and for $0.9 \leq \delta < 1$ when $n = 7$, the proposed chart also performs better than the standard chart. Table 1 points out that the larger n results in a better performance of the chart in both improvement and deterioration cases. Moreover, with an increase in $n$, the range of the downward shifts becomes shorter in which the proposed chart is inferior to the standard chart. The study clearly indicates that the performance of the chart using the RS can be improved with choosing larger $ASS_0$ value which supports the existing research's findings.

## 4. Design of the Phase II ARL-unbiased $S^2$-chart under repetitive sampling

In this section, we modify the control limits of the proposed ARL-biased $S^2$-chart under the RS so that the chart is ARL-unbiased and attains the desired IC performance. To construct the ARL-

unbiased $S^2$-chart under the RS, we introduce the design constants $\gamma$, $\alpha_1'$ and $\alpha_2'$, so that the modified outer and inner control limits under the RS are obtained as follows.

$$\mathrm{LCL}'_{\mathrm{RS}} = \frac{\sigma_0^2}{n-1}\chi^2_{\gamma\alpha_1',n-1} = \frac{\sigma_0^2}{n-1}B_1' \quad \text{and} \quad \mathrm{UCL}'_{\mathrm{RS}} = \frac{\sigma_0^2}{n-1}\chi^2_{1-\alpha_1',n-1} = \frac{\sigma_0^2}{n-1}B_2' \tag{10a}$$

$$\mathrm{LRL}'_{\mathrm{RS}} = \frac{\sigma_0^2}{n-1}\chi^2_{\gamma\alpha_2',n-1} = \frac{\sigma_0^2}{n-1}R_1' \quad \text{and} \quad \mathrm{URL}'_{\mathrm{RS}} = \frac{\sigma_0^2}{n-1}\chi^2_{1-\alpha_2',n-1} = \frac{\sigma_0^2}{n-1}R_2' \tag{10b}$$

where the constants $\alpha_1', \alpha_2'$ $(0 < \alpha_1' \le \alpha_2' < 1)$ are determined to keep the IC performance at a desired level and $\gamma$ is obtained to eliminate the bias in the ARL function. For $\gamma = 1$, the chart reduces to the ARL-biased $S^2$-chart under the RS. Also, $B_1' = \chi^2_{\gamma\alpha_1',n-1}, B_2' = \chi^2_{1-\alpha_1',n-1}$, $R_1' = \chi^2_{\gamma\alpha_2',n-1}$ and $R_2' = \chi^2_{1-\alpha_2',n-1}$, respectively. To obtain the ARL from Equation (7) and ASS from Equation (8) for the ARL-unbiased $S^2$-chart under the RS, the probabilities $p_a$, $p_b$, $p_c$, $p_d$, $p_e$ and $p_f$ can be obtained from the set of Equations (5), respectively by replacing $B_1, B_2, R_1, R_2$ with $B_1', B_2', R_1', R_2'$, respectively.

To construct the control limits for an ARL-unbiased $S^2$-chart under RS, we set (i) IC ARL equals to the nominal $\mathrm{ARL}_0$, (Equation 11a) (ii) IC ASS equals to desired $\mathrm{ASS}_0$ (Equation 11b), and (iii) the first derivative of the ARL function with respect to $\delta$ at $\delta = 1$ equal to zero so that the ARL function is maximized at the IC state of the process, i.e., $\delta$=1, (Equation 11c). Thus, the design constants $\gamma, \alpha_1'$ and $\alpha_2'$ can be obtained by solving the following set of Equations.

$$\mathrm{ARL}_{\mathrm{RS}}(1) = \mathrm{ARL}_0 \tag{11a}$$

$$\mathrm{ASS}_{\mathrm{RS}}(1) = \mathrm{ASS}_0 \tag{11b}$$

$$\frac{\mathrm{d}}{\mathrm{d}\delta}\mathrm{ARL}_{\mathrm{RS}}(\delta)|_{\delta=1} = 0 \tag{11c}$$

where, $\mathrm{ARL}_{\mathrm{RS}}(\delta)|_{\delta=1} = \frac{\left(p_a(\delta)+p_f(\delta)\right)\left[-p_b'(\delta)-p_e'(\delta)\right]-\left(1-p_b(\delta)-p_e(\delta)\right)\left[p_a'(\delta)-p_f'(\delta)\right]}{(p_a(\delta)+p_f(\delta))^2}$ with $p_a'(\delta)|_{\delta=1} = -\left(-\frac{B_1}{\delta^2}\right)f_{\chi^2_{n-1}}\left(\frac{B_1}{\delta}\right)$, $p_b'(\delta)|_{\delta=1} = \left(-\frac{B_1}{\delta^2}\right)f_{\chi^2_{n-1}}\left(\frac{B_1}{\delta}\right) - \left(-\frac{R_1}{\delta^2}\right)f_{\chi^2_{n-1}}\left(\frac{R_1}{\delta}\right)$, $p_e'(\delta)|_{\delta=1} = \left(-\frac{R_2}{\delta^2}\right)f_{\chi^2_{n-1}}\left(\frac{R_2}{\delta}\right) - \left(-\frac{B_2}{\delta^2}\right)f_{\chi^2_{n-1}}\left(\frac{B_2}{\delta}\right)$ and $p_f'(\delta)|_{\delta=1} = \left(-\frac{B_2}{\delta^2}\right)f_{\chi^2_{n-1}}\left(\frac{B_2}{\delta}\right)$. Since the values of the design constants cannot be obtained analytically, we used the numerical iterative procedure in 'R' software to solve them.

Note that for $\alpha_1' = \alpha_2'$, the ARL-unbiased $S^2$-chart under the RS reduces to the ARL-unbiased $S^2$-chart under the SS and consequently, $\mathrm{UCL}'_{\mathrm{RS}} = \mathrm{URL}'_{\mathrm{RS}}$ and $\mathrm{LCL}'_{\mathrm{RS}} = \mathrm{LRL}'_{\mathrm{RS}}$. Therefore, the control limits of the ARL-unbiased $S^2$-chart under SS can be obtained as follows.

$$\mathrm{LCL}'_{\mathrm{RS}} = \frac{\sigma_0^2}{n-1}B_1' = \mathrm{LCL}' \quad \text{and} \quad \mathrm{UCL}'_{\mathrm{RS}} = \frac{\sigma_0^2}{n-1}B_2' = \mathrm{UCL}' \tag{12}$$

where the constants $\alpha_1'$ $(0 < \alpha_1' < 1)$ and $\gamma \ge 1$ can be obtained to solve the following conditions. Please see also, Knoth and Morais (2015).

$$\mathrm{ARL}(1) = \mathrm{ARL}_0 \tag{13a}$$

$$\frac{\mathrm{d}}{\mathrm{d}\delta}\mathrm{ARL}(\delta)|_{\delta=1} = 0 \tag{13b}$$

where $\frac{\mathrm{d}}{\mathrm{d}\delta}\mathrm{ARL}(\delta)|_{\delta=1} = \left[\left(-\frac{B_2'}{\delta^2}\right)f_{\chi^2_{n-1}}\left(\frac{B_2'}{\delta}\right) - \left(-\frac{B_1'}{\delta^2}\right)f_{\chi^2_{n-1}}\left(\frac{B_1'}{\delta}\right)\right] / \left[1 + F_{\chi^2_{n-1}}\left(\frac{B_1'}{\delta}\right) - F_{\chi^2_{n-1}}\left(\frac{B_2'}{\delta}\right)\right]^2$. Once we obtain the design constants, we can calculate the control limits of the ARL-unbiased $S^2$-chart using Equation (12).

## 5. Performance comparison of the proposed ARL-unbiased $S^2$-chart under repetitive sampling and standard ARL-unbiased $S^2$-chart

To evaluate the proposed ARL-unbiased $S^2$-chart under the RS and compare with the standard ARL unbiased $S^2$-chart, we obtain the control limits for $ARL_0 = 370$ and $ASS_0 = 4.4, 4.8$ (for $n = 4$) and 7.7, 8.4 (for $n = 7$). The corresponding ARL and ASS values for both charts are reported in Table 2 for different $\delta$ values. It can be observed that the OOC ARL values are smaller than the IC ARL for all shift sizes which guarantees a higher chance of detecting shifts in the process variance than giving a false alarm. The charts under the RS outperform the standard ARL-unbiased $S^2$-chart in terms of smaller OOC ARL values. For example, when $n = 4, \delta = 0.7$, the standard ARL-unbiased $S^2$-chart has ARL value 254.70 whereas it is 245.72 for the proposed chart with $ASS_0 = 4.4$ and 238.35 with

$ASS_0 = 4.8$. It is worth to note that unlike the ARL-biased chart, the ARL-unbiased chart with the RS performs better than the corresponding ARL unbiased $S^2$-chart for all shifts. Moreover, the larger $n$ and $ASS_0$ result in an improved performance. The design of the proposed chart is flexible, and a user can design at his/her own choice how much he/she is willing to pay the price in terms of large $ASS_0$ to get the OOC signal quickly. It is worth mentioning that the chart becomes inferior to the ARL-biased $S^2$-chart in the deterioration case. It may seem unreasonable because one wish to have a chart which is able to detect the situations that are responsible for bad quality items. Final choice, however, is with the management. The present study provides choices to the user/management that he/she can choose an appropriate chart in his/her favorable conditions.

**Table 2:** *Un-biased performance of the equal-tailed $S^2$-chart under SS and RS using the metric ARL and ASS for nominal $ARL_0 = 370$, $ASS_0 = 4.4, 4.8$ at $n = 4$ and $ASS_0 = 7.7, 8.4$ at n=7, respectively.*

| | $n = 4$ | | | | | | $n = 7$ | | | | | |
|---|---|---|---|---|---|---|---|---|---|---|---|---|
| | ARL-unbiased $S^2$ | | Proposed ARL-unbiased chart | | | | ARL-unbiased $S^2$ | | Proposed ARL-unbiased chart | | | |
| | | | ASS = 4.4 | | ASS = 4.8 | | | | ASS = 7.7 | | ASS = 8.4 | |
| $\delta$ | ARL | ASS | ARL | ASS | ARL | ASS | ARL | ASS | ARL | ASS | ARL | ASS |
| **0.1** | 15.36 | 4.00 | 3.99 | 16.87 | 1.96 | 37.27 | 2.22 | 7.00 | 1.01 | 16.19 | 1.00 | 17.12 |
| **0.3** | 73.38 | 4.00 | 53.57 | 6.04 | 41.87 | 8.43 | 19.51 | 7.00 | 9.11 | 16.32 | 5.96 | 26.96 |
| **0.5** | 155.25 | 4.00 | 138.82 | 4.93 | 126.79 | 5.90 | 71.11 | 7.00 | 55.60 | 9.82 | 47.33 | 12.57 |
| **0.7** | 254.70 | 4.00 | 245.72 | 4.57 | 238.35 | 5.15 | 175.64 | 7.00 | 163.42 | 8.29 | 155.56 | 9.51 |
| **0.9** | 351.05 | 4.00 | 349.52 | 4.43 | 347.91 | 4.86 | 330.21 | 7.00 | 327.60 | 7.78 | 325.74 | 8.56 |
| **1** | 370.00 | 4.00 | 369.85 | 4.40 | 369.92 | 4.80 | 370.00 | 7.00 | 369.98 | 7.70 | 369.91 | 8.40 |
| **1.1** | 348.38 | 4.00 | 346.90 | 4.39 | 346.79 | 4.77 | 325.17 | 7.00 | 322.80 | 7.69 | 321.15 | 8.37 |
| **1.3** | 224.97 | 4.00 | 218.74 | 4.41 | 216.02 | 4.79 | 149.61 | 7.00 | 142.72 | 7.84 | 138.79 | 8.55 |
| **1.5** | 122.57 | 4.00 | 115.69 | 4.48 | 112.55 | 4.87 | 64.36 | 7.00 | 58.41 | 8.13 | 55.59 | 8.95 |
| **1.7** | 69.44 | 4.00 | 63.64 | 4.57 | 61.12 | 4.99 | 32.50 | 7.00 | 27.97 | 8.50 | 26.13 | 9.46 |
| **3** | 9.21 | 4.00 | 7.29 | 5.17 | 6.71 | 5.75 | 4.07 | 7.00 | 2.87 | 10.15 | 2.58 | 11.46 |
| **4** | 4.81 | 4.00 | 3.65 | 5.37 | 3.35 | 5.95 | 2.32 | 7.00 | 1.67 | 9.84 | 1.55 | 10.75 |
| $k$ | 5.821054 | | 5.674593 | | 5.614001 | | 3.556330 | | 3.495460 | | 3.435879 | |
| $\alpha_1$ | 0.000396 | | 0.000368 | | 0.000341 | | 0.000593 | | 0.000547 | | 0.000508 | |
| $\alpha_2$ | | | 0.013988 | | 0.025540 | | | | 0.020769 | | 0.038080 | |

## 6. Example

To illustrate an application of the proposed ARL-biased and -unbiased $S^2$-chart using the RS, we use data considered in a case study of syringes with a self-contained, single dose of an injectable drug produced by a pharmaceutical company. The conclusions of the case study and associated data have published in Franklin and Mukherjee [10]. The critical quality characteristic was the length at which the cap of the syringe was tacked. For further details, we refer the interested readers to follow Franklin and Mukherjee [10]. Based on the capability analysis with $C_{pk} = 1.04$, the management determined that the process was minimally capable and susceptible to producing the length desired. Therefore, it was decided to monitor the process via control charts to find any reasonable cause(s).

To monitor the process under consideration, the case study considered total 47 samples each of size 5 which are reported in Table 2 of Frankline and Mukherjee [10]. In their study, the $R$-chart was used to monitor the process variability. The quality practitioner used the first 15 points to construct the control limits of the $\bar{X}$- and $R$- charts and plotted these 15 points on the charts. The charts show that the process is OOC in both centre and variation as well. However, these OOC signals were not noticed. We use the $S^2$- chart instead of $R$-chart and find that the $S^2$-chart does not give any OOC signal implying that the variability is IC. The next 15 samples were collected for phase II monitoring, and it was noticed that the caps were not perfectly tacked. Thus, the technician was called for the adjustments. Taking the first attempt of the machine adjustment into consideration, 31st sample was collected and observed that still the machine was not at its targeted position and to the next, second attempt were made to adjust the machine. Sample number 32nd were collected and plotted on the R chart to observe the adjustment effect. Quality practitioner observed that the second adjustment was also no better and the technician called for the third time. The third try was successful in the sense that the next 15 samples collected and plotted, and no point was beyond the control limits, and no action was taken.

However, a careful examination of both charts indicates that the process is not IC. To examine the sensitivity of variation, here, $S^2$-chart under RS (proposed chart) has been used instead of R-chart. For this purpose, we implement the ARL-biased and -unbiased charts design under the RS with nominal $(\mathrm{ARL}_0,\ \mathrm{ASS}_0) = (370.4, 5.5)$ for $n = 5$. The estimates from the first 15 samples were used to construct the control limits of the proposed $S^2$-chart under the RS. We get variance estimate $\sigma^2 = 0.000134$. The set of control limits $(\mathrm{LCL}_{RS}, \mathrm{UCL}_{RS})$ and the repetitive limit $(\mathrm{LRL}_{RS}, \mathrm{URL}_{RS})$ of the ARL-biased and -unbiased $S^2$-charts under the RS are found to be $3.37 \times 10^{-6}, 6.03 \times 10^{-4}$ and $(2.29 \times 10^{-5},\ 3.23 \times 10^{-4})$ and $(4.34 \times 10^{-6},\ 6.79 \times 10^{-4})$ and $(3.04 \times 10^{-5},\ 4.04 \times 10^{-4})$, respectively, which are depicted in Figure 1 with the $\mathrm{CL} = 1.34 \times 10^{-4}$. For the better visualization, we have taken the y-axis on log scale. Red and dashed lines represent the control limits of the ARL-unbiased $S^2$-chart under RS, whereas black and dashed lines represent the control limits of the ARL-biased $S^2$-chart under the RS. It can be seen from Figure 1 (Panels 2 and 3) that unlike the $R$-chart, both ARL-biased and -unbiased $S^2$-charts under the RS produce OOC signals. Thus, the process for the first 15 samples may be considered IC. The next 17 sample points clearly indicate the signal at the points 23 and 28. After the adjustment, the proposed chart also gives a signal at the 41st point. In the case study, the quality practitioner observed that the process was OOC signal based on the supplementary runs rules. However, a less qualified operator overlooked these non-random patterns. The proposed chart gives more objective assessment to decide the OOC signal because the points are lying below the control limits.

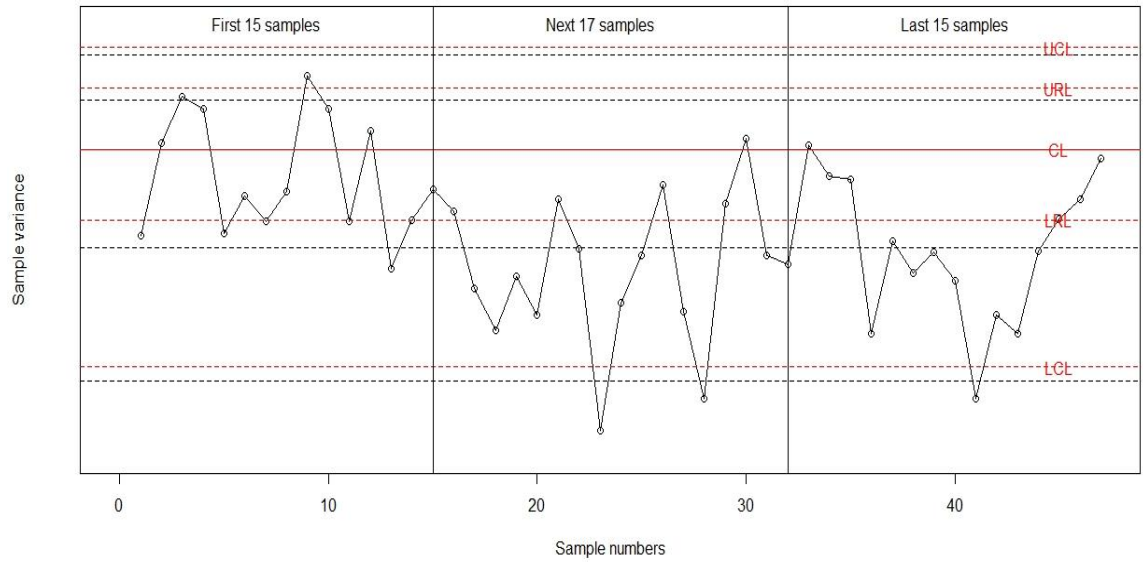


**Figure 1:** *The ARL-unbiased $S^2$-chart under the RS (red dashed lines) and ARL-biased $S^2$-chart under the RS (black dashed lines).*

## 7. Conclusion

In this paper, we consider the ARL-biased (equal-tailed) and -unbiased $S^2$-charts to monitor the changes (both upward and downward) in the process variance. The study shows that the ability of both charts to early detect changes can be enhanced by using the RS with maintaining simplicity of design and operation and features of the Shewhart's type charts. The ARL-biased and -unbiased $S^2$-charts using the RS perform better than their counterparts ARL-biased and -unbiased $S^2$-charts under the SS. The ARL-biased chart using the RS outperforms the ARL-unbiased chart using the RS in detecting an increase in the variance, though the latter ensures an early detection of both downward and upward shifts than it raises the false alarm. The study provides alternatives of choosing their designs according to their need. Indeed, if the management is aspiring for a continual improvement of the process, he may opt the ARL-unbiased $S^2$-chart under the RS.

Further, many research topics maybe of interest as a follow-up. The present study considers the case when the process variance is known, which may not be suitable in some real applications. It is well accepted that the parameter estimation affects the chart's performance in a negative way which also needs to be investigated. Following the recent literature, the conditional and unconditional performance of the proposed charts can be investigated given a Phase I sample. Finally, all the calculations are performed using the R statistical software and the programs are available from the authors on request.

## References

[1] Ahmad, L., Aslam, M., and Jun, C. H. (2014). Designing of X-bar control charts based on process capability index using repetitive sampling. *Transactions of the Institute of Measurement and Control*, 36: 367-374.

[2] Alevizakos, V., Chatterjee, K., Koukouvinos, C., and Lappa, A. (2023). The effect of parameters estimation on the performance of variables control charts under repetitive sampling. *Communications in Statistics-Theory and Methods*, 52:2379-2401.

[3] Aslam, M. (2019). Control chart for variance using repetitive sampling under neutrosophic statistical interval system. *IEEE Access*, 7:25253-25262.

[4] Aslam, M., Azam, M., and Jun, C. H. (2014). New attributes and variables control charts under repetitive sampling. *Industrial Engineering and Management Systems*, 13:101-106.

[5] Aslam, M., Khan, N., and Jun, C. H. (2015). A new $S^2$ control chart using repetitive sampling. *Journal of Applied Statistics*, 42:2485-2496.

[6] Aslam, M., Khan, N., Azam, M., and Jun, C. H. (2014). Designing of a new monitoring t-chart using repetitive sampling. *Information sciences*, 269:210-216.

[7] Castagliola P, Celano G, and Fichera S (2009). A new CUSUM-$S^2$ control chart for monitoring the process variance. *Journal of Quality in Maintenance Engineering*, 0:0-0.

[8] Chang, T. C., and Gan, F. F. (1994). Optimal designs of one-sided EWMA charts for monitoring a process variance. *Journal of statistical Computation and Simulation*, 49:33-48.

[9] Chang, T. C., and Gan, F. F. (1995). A cumulative sum control chart for monitoring process variance. *Journal of Quality Technology*, 27:109-119.

[10] Franklin, L. A., and Mukherjee, S. N. (1999). An SPC case study on stabilizing syringe lengths. *Quality Engineering*, 12:65-71.

[11] He, D., and Grigoryan, A. (2002). Construction of double sampling s-control charts for agile manufacturing. *Quality and reliability engineering international*, 18:343-355.

[12] Khoo, M. B. (2004). $S^2$ control chart based on double sampling. *International Journal of Pure and Applied Mathematics*, 13:249-258.

[13] Knoth S and Morais M C (2015). On ARL-unbiased control charts. In *Frontiers in Statistical Quality Control*, 11:95-117.

[14] Lawson, J. (2019). Phase II monitoring of variability using Cusum and EWMA charts with individual observations. *Quality Engineering*, 31:417-429.

[15] Montgomery, D. C. (2020). *Introduction to statistical quality control*. John Wiley & Sons.

[16] Pignatiello Jr, J. J., Acosta-Mejia, C. A., and Rao, B. V. (1995). The performance of control charts for monitoring process dispersion. In *Proceedings of the 4th Industrial Engineering Research Conference*, 0:320-328

[17] Sarmiento, M. G., Chakraborti, S., and Epprecht, E. K. (2018). Exact two-sided statistical tolerance limits for sample variances. *Quality and Reliability Engineering International*, 34:1238-1253.

[18] Sherman, R. E. (1965). Design and evaluation of a repetitive group sampling plan. *Technometrics*, 7:11-21.

[19] Singh, T., and Kumar, N. (2022). Improved Phase II exponential chart under repetitive sampling. *International Journal of Agricultural and Statistical Sciences*, 0:0-0.

[20] Zhang, L., Bebbington, M. S., Lai, C. D., and Govindaraju, K. (2005). On statistical design of the $S^2$ control chart. *Communications in Statistics-theory and Methods*, 34:229-244.